



ELSEVIER

Contents lists available at SciVerse ScienceDirect

# Applied Mathematical Modelling

journal homepage: [www.elsevier.com/locate/apm](http://www.elsevier.com/locate/apm)

## Repeated Richardson extrapolation applied to the two-dimensional Laplace equation using triangular and square grids

C.H. Marchi <sup>a,\*</sup>, L.K. Araki <sup>b</sup>, A.C. Alves <sup>c</sup>, R. Suero <sup>d</sup>, S.F.T. Gonçalves <sup>b</sup>, M.A.V. Pinto <sup>b</sup><sup>a</sup> Federal University of Paraná (UFPR), Department of Mechanical Engineering (DEMEC), Zip Code: 81531-980, Caixa postal 19040, Curitiba, PR, Brazil<sup>b</sup> Federal University of Paraná (UFPR), Department of Mechanical Engineering (DEMEC), Zip Code: 81531-980, Curitiba, PR, Brazil<sup>c</sup> Positivo University (UP), Sector of Exact Sciences and Technology, Zip Code: 81280-330, 5300 Professor Pedro Viriato Parigot de Souza Street, Curitiba, PR, Brazil<sup>d</sup> Federal Institute of Paraná (IFPR), Campus of Paranaguá, Zip Code: 83215-750, 453 Antonio Carlos Rodrigues Street, Paranaguá, PR, Brazil

### ARTICLE INFO

#### Article history:

Received 7 October 2011

Received in revised form 24 August 2012

Accepted 25 September 2012

Available online 6 October 2012

#### Keywords:

Richardson extrapolation

Discretization error

Triangular grid

Finite volume

Order of accuracy

Verification

### ABSTRACT

The focus of this work is to verify the efficiency of the Repeated Richardson Extrapolation (RRE) to reduce the discretization error in a triangular grid and to compare the result to the one obtained for a square grid for the two-dimensional Laplace equation. Two different geometries were employed: the first one, a unitary square domain, was discretized into a square or triangular grid; and the second, a half square triangle, was discretized into a triangular grid. The methodology employed used the following conditions: the finite volume method, uniform grids, second-order accurate approximations, several variables of interest, Dirichlet boundary conditions, grids with up to 16,777,216 nodes for the square domain and up to 2097,152 nodes for the half square triangle domain, multigrid method, double precision, up to eleven Richardson extrapolations for the first domain and up to ten Richardson extrapolations for the second domain. It was verified that (1) RRE is efficient in reducing the discretization error in a triangular grid, achieving an effective order of approximately 11 for all the variables of interest for the first geometry; (2) for the same number of nodes and with or without RRE, the discretization error is smaller in a square grid than in a triangular grid; and (3) the magnitude of the numerical error reduction depends on, among other factors, the variable of interest and the domain geometry.

© 2012 Elsevier Inc. All rights reserved.

## 1. Introduction

The continuous improvement of computer resources had led to the ability to describe natural phenomena at previously unimaginable scales and this ability has been a focus of research for the computational sciences and engineering, especially in the last 20 years [1]. To achieve accurate results, however, some verification procedures are required. Most of these procedures are based on Richardson extrapolation [2,3]. One in particular, called Repeated Richardson Extrapolation (RRE), Recursive Richardson Extrapolation (RRE) or Multiple Richardson Extrapolation (MRE) is used in the current work on two grid types: triangular and square control volumes.

The numerical error  $E(\phi)$  related to the numerical solution  $\phi$  can be evaluated by the following expression:

$$E(\phi) = \Phi - \phi, \quad (1)$$

where  $\Phi$  is the exact analytical solution. There are four sources of numerical error: truncation, iteration, round-off and programing errors [4]. When the numerical error is solely due to truncation, it is called discretization error [5].

\* Corresponding author. Tel.: +55 41 33613126; fax: +55 41 33613701.

E-mail addresses: [marchi@ufpr.br](mailto:marchi@ufpr.br), [machi@pq.cnpq.br](mailto:machi@pq.cnpq.br) (C.H. Marchi), [lucaraki@ufpr.br](mailto:lucaraki@ufpr.br) (L.K. Araki), [aalves@up.com.br](mailto:aalves@up.com.br) (A.C. Alves), [roberta.suero@ifpr.edu.br](mailto:roberta.suero@ifpr.edu.br) (R. Suero), [simone.tg@ufpr.br](mailto:simone.tg@ufpr.br) (S.F.T. Gonçalves), [marcio\\_villela@ufpr.br](mailto:marcio_villela@ufpr.br) (M.A.V. Pinto).

Procedures for estimating discretization error were first proposed by Richardson at the beginning of the 20th century [2,3]. In addition to the common use of Richardson extrapolation as an error estimator, the technique can also be used to reduce discretization error, such as that associated with the two-dimensional heat diffusion problem – an application to which Richardson himself investigated [3]. In this case, Richardson extrapolations were employed recursively for two grid levels, providing more-accurate results. Other authors [6–8] also employed Richardson extrapolations recursively for a higher number of grid levels (with a maximum of four), intending to reduce the discretization errors in CFD (Computational Fluid Dynamics) problems. More common is the use of only one Richardson extrapolation for the reduction of discretization error, as demonstrated by Wang and Zhang [9,10] and Ma and Ge [11].

Marchi et al. [12] and Marchi and Germer [13], however, employed Richardson extrapolations recursively for several grid levels through a process called RRE for a two-dimensional Laplace equation and one-dimensional advection-diffusion equation, respectively, using structured grids. In both cases, discretization errors were substantially reduced. According to these works, RRE should be used in the following ways: (1) for a given discretization error magnitude, it can reduce the computational requirements by employing coarser grids; or (2) for a given grid, it can considerably reduce the magnitude of the discretization errors to obtain *benchmark* results.

Richardson extrapolations have also been applied to adaptive grids. Ouellet and Bui [14] employed Richardson extrapolation to increase the accuracy and refine a grid automatically, if necessary, for the discretization of industrial thermal problems based on an Euler central differentiation scheme using backward differentiation. Biswas et al. [15] controlled the grid motion and refinement using local indicators, which were estimates of the local discretization error. *A posteriori* estimates of the local discretization error obtained by Richardson extrapolation were used as refinement indicators as well as motion indicators. Singularity problems were studied by Koestler and Ruede [16] in which only minor modifications to both the discretization and solver were necessary to obtain the same asymptotic accuracy and efficiency as those for regular solutions. The authors showed that it is possible to integrate these techniques into a multigrid solver with additional techniques to improve accuracy, as observed with the use of Richardson extrapolations. Kamkar et al. [17] described a Cartesian-based adaptive mesh refinement approach applied to vortex-dominated flows. Richardson extrapolation was proposed to assess the local error and terminate the mesh refinement once an adequate error reduction was achieved. Based on these cited studies, it is expected that the extension of RRE to adaptive grids is immediate.

The aim of this work is to investigate the use of RRE to reduce the discretization errors of the two-dimensional Laplace equation. Two different geometries are employed: the first one, a unitary square domain, is discretized into an isosceles right-triangular grid, for which the results are compared to those obtained on square volume grids; and the second one, a half square triangle, is only discretized into an isosceles right-triangular grid. Triangular volumes are usually related to unstructured grids, which constitute the most general grid arrangement for more complex geometries [18]. Nevertheless, Juretić and Gosman [19] analyzed, both theoretically and numerically, triangular, square and hexagonal grids, observing that triangular grids presented the worst performance, taking into account the discretization errors. This motivates the study of whether RRE can be employed on triangular grids for the reduction of the associated discretization error and, in the affirmative case, how effective this methodology is. The Laplace equation was chosen in the current work due to its simplicity and because, for the studied problem, it presents an analytical solution that allows for the evaluation of the true numerical errors for all the variables of interest. The study of RRE to reduce the discretization errors on triangular grids is also motivated by the absence of studies involving triangular grids and Richardson extrapolations: works such as Jyotsna and Vanka [20], in which Richardson extrapolations were employed to obtain more-accurate results for the velocity pattern using triangular grids are still exceptions.

## 2. Mathematical model

Given that the objective of this study is to show how RRE could reduce the discretization error in both grid types (structured and unstructured ones), it seems reasonable to choose a simple problem, with a simple geometry to analyze specifically the effects of the RRE methodology. More complex problems imply the presence of more complex terms (derivatives, products of variables, nonlinearities), whose numerical approximations could mask the effects of RRE by, for example, the degeneration of the orders of the discretization error. For these reasons, a unitary square domain is employed to provide numerical results for both structured and unstructured discretization methodologies. In Section 4.5, however, a second domain geometry is employed: a half square triangle, which is discretized into only a triangular grid. This second geometry is used to verify whether the numerical results obtained for the first geometry can be applied to others.

The mathematical model for the first domain geometry is related to the two-dimensional Laplace equation with Dirichlet boundary conditions:

$$\begin{cases} \frac{\partial^2 T}{\partial x^2} + \frac{\partial^2 T}{\partial y^2} = 0, & 0 < x, y < 1, \\ T(x, 1) = \sin(\pi x), \quad T(0, y) = T(1, y) = T(x, 0) = 0, \end{cases} \quad (2)$$

where  $x$  and  $y$  are the spatial coordinates and  $T$  is the temperature. This equation can be physically related to the heat diffusion problem on a two-dimensional plate in the steady state with constant thermal properties and the absence of heat generation [21], whose analytical solution is given by  $T(x, y) = \sin(\pi x) \sinh(\pi y) / \sinh(\pi)$ .

The variables of interest include the following: (1) the temperature at the domain center ( $T_c$ ), in other words, the temperature at position  $x = 1/2$  and  $y = 1/2$ ; (2) the average temperature ( $T_m$ ) of the whole domain; and the heat transfer rates at the four boundaries, namely (3)  $y = 1$  ( $Q_n$ ), (4)  $y = 0$  ( $Q_s$ ), (5)  $x = 1$  ( $Q_e$ ) and (6)  $x = 0$  ( $Q_w$ ). The variables  $T_m$ ,  $Q_s$  and  $Q_e$  are defined by the following expressions:

$$T_m = \frac{1}{L_x L_y} \int_0^{L_y} \int_0^{L_x} T(x, y) dx dy, \quad Q_s = -kz \int_0^{L_x} \left( \frac{\partial T}{\partial y} \right)_{y=0} dx, \quad Q_e = -kz \int_0^{L_y} \left( \frac{\partial T}{\partial x} \right)_{x=1} dy, \quad (3)$$

where  $L_x = L_y = 1$  are the lengths of the domain in the  $x$  and  $y$  directions, respectively;  $z = 1$  is the depth of the domain in the  $z$  direction; and  $k$  is the thermal conductivity, which is assumed to have unitary value.  $Q_n$  and  $Q_w$  are defined analogously to  $Q_e$  and  $Q_s$ . The justification for the choice of these variables is presented in the next section.

### 3. Numerical model

#### 3.1. Numerical solutions without RRE

The unitary side square domain is discretized using the finite volume method [5,18] into both triangular and square grids (Fig. 1). While the methodology applied to square grids is that related to structured grids, on triangular grids the methodology is the same as that employed on unstructured ones. There are two ways of defining control volumes on unstructured grids: (i) as cell-centered control volumes and (ii) as vertex-centered control volumes. Both are used in practice [18]. The choice to use the cell-centered method, however, is made for the following reasons: (i) all volumes in this method present the same shape and size; and (ii) on square grids, using the cell-centered method is common practice. Based on these two reasons, the cell-centered method allows for a better comparison between triangular and square grids. Numerical approximations on both grid types are performed by using the Central Differencing Scheme (CDS).

For the unstructured grid methodology (triangular grids), integration is performed over a given control volume:

$$\int_{CV} \nabla \cdot (\nabla T) dV = 0. \quad (4)$$

Once the control volume surface is divided into line segments, and recalling the Gauss's Divergence Theorem, the following expression is derived:

$$\sum_{\text{all } i \text{ surfaces}} [\vec{n}_i \cdot (\nabla T) \Delta A_i] = 0, \quad (5)$$

where  $\vec{n}_i = (\Delta y / \Delta A_i) \hat{i} - (\Delta x / \Delta A_i) \hat{j}$  is the vector normal to the  $i$  surface, whose area is given by  $\Delta A_i$ , which is numerically evaluated by  $\Delta A_i = \sqrt{(\Delta x)^2 + (\Delta y)^2}$ , where  $\Delta x = x_b - x_a$  and  $\Delta y = y_b - y_a$  (see Fig. 2, considering the  $ab$  face).

According to Eq. (5), it is essential to evaluate the inner product between each polygon surface normal vector and the temperature gradient along this surface. To evaluate the summand of Eq. (5), the temperature gradient should be approximated by CDS along the line that connects two neighboring centroids – line  $PA$  in Fig. 2. However, if, as is typically the case, the normal vector and the temperature gradient are not parallel, the discretization of Eq. (5) is performed by introducing a term known as cross-diffusion, which is evaluated according to the expression developed by Mathur and Murthy [22] and results in the following:

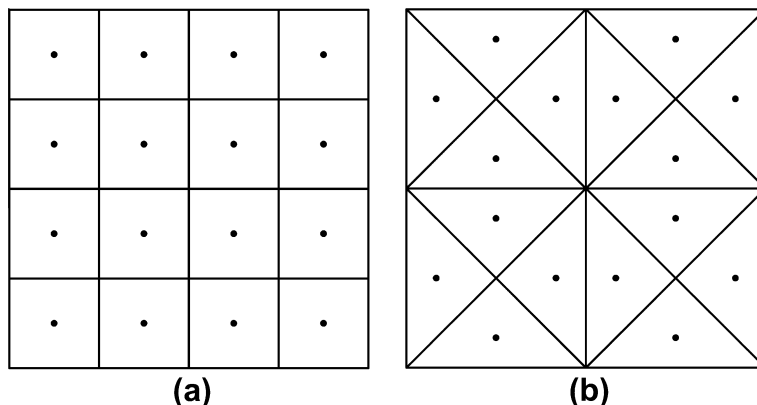
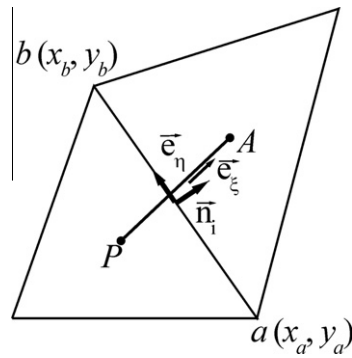


Fig. 1. (a) Square and (b) isosceles right-triangular grids with 16 control volumes. Unitary square domain.



**Fig. 2.** Definition of the unit vectors for the discretization process. On this grid, there is a misalignment between the midpoint of the triangle face  $ab$  and the line  $PA$  that connects the two centroids.

$$\vec{n}_i \cdot (\nabla T) \Delta A_i = \frac{\vec{n}_i \cdot \vec{n}_i}{\vec{n}_i \cdot \vec{e}_\zeta} \frac{T_A - T_P}{\Delta \zeta} \Delta A_i - \frac{\vec{e}_\zeta \cdot \vec{e}_\eta}{\vec{n}_i \cdot \vec{e}_\zeta} \frac{T_b - T_a}{\Delta \eta} \Delta A_i, \tag{6}$$

where  $\vec{e}_\zeta$  is the unit vector along the line that connects the centroids  $P$  and  $A$ ;  $\Delta \zeta$  is the distance between two neighboring centroids  $P$  and  $A$ ;  $\vec{e}_\eta$  is the unit vector along the line  $ab$  (Fig. 2), which is the common triangle side;  $\Delta \eta$  is the distance between the vertices  $a$  and  $b$  (and is numerically equal to  $\Delta A_i$ ); and  $T_a$  and  $T_b$  are the values of the temperature evaluated at the  $a$  and  $b$  vertices, respectively. The first term on the right side of Eq. (6) is known as the direct gradient term, and the second term is the cross-diffusion term.

In the current work, the previous procedure, however, is facilitated by two facts related to the grids' construction: (1) both the normal and the temperature gradient vectors are always parallel; and (2) the intersection point of the line that connects two neighboring centroids and the triangle face splits this line exactly into two equal parts. Based on these facts, (1) the cross-diffusion term of Eq. (6) is null if the unit vectors  $\vec{e}_\zeta$  and  $\vec{e}_\eta$  are perpendicular; and (2) CDS, which is applied to the evaluation of the derivatives of the direct gradient term, is expected to present a second order of accuracy when applied exactly at the midpoint of line that connects the centroids. Substituting Eq. (6) into Eq. (5) and recalling the foregoing remarks, the following expression is obtained for an inner control volume:

$$\sum_{\text{all } i \text{ surfaces}} \left[ \frac{T_A - T_P}{\Delta \zeta_A} \Delta A_i \right] = 0, \tag{7}$$

where  $P$  represents the control volume in which the integration process takes place;  $A$  represents each neighboring centroid, whose  $i$  face is the common face with  $P$ ;  $\Delta A_i$  is the area of the common  $i$  face; and  $\Delta \zeta_A$  is the distance between centroids  $P$  and  $A$ .

Boundary conditions are applied using the ghost-cells technique. According to this technique, ghost-cells are placed out of the real domain and each cell is a mirrored image of an inner control volume placed at the domain boundary. It is important to note that for the chosen triangular grids, the line that connects the centroid of the real volume to the centroid of the ghost-cell intersects the triangle face exactly at its midpoint. This fact avoids undesired discretization errors from arising for the boundary conditions with respect to the grid skewness [18,19], which consists in the misalignment between the midpoint of the triangle face and the line that connects the centroids. According to the ghost-cell technique, if the boundary conditions are of the Dirichlet type, the value of the boundary condition is evaluated at the face midpoint and is equal to the average of the values attributed to the real and the ghost-cell centroids.

On square grids, the methodology employed is that related to structured grids [18]. For each coordinate direction, CDS is used to evaluate the derivatives on the control volume faces. Boundary conditions are also applied by using the ghost-cells technique.

The use of the CDS for the discretization of a mathematical model is based on the results previously reported by Marchi and Germer [13]. They studied the one-dimensional advection-diffusion problem and employed ten different pairs of numerical approximations for the discretization process, including first-order (UDS), second-order (CDS, UDS-2, WUDS), third-order (Quick) and fourth-order (CDS-4) approximations, resulting in first-, second- and third-order numerical models. According to the numerical results, it was observed that using the CDS was the best approach to apply the RRE methodology, even when the discretization error for the Quick/CDS-4 model presented the smallest discretization error before the application of RRE.

To speed up the convergence of the numerical codes, two different multigrid methods were employed: on triangular grids, an algebraic multigrid (AMG) algorithm adapted from Ruge and Stüben [23] was employed; and on square grids, a geometric multigrid (GMG) algorithm was used [24,25]. The AMG features employed to achieve the numerical results include the following: correction scheme (CS) [23,26,27]; V-cycle; a connection strength parameter ( $\theta$ ) equal to 0.25; and a parameter describing the strong dependence on the coarser grid ( $\epsilon$ ) equal to 0.35. Otherwise, for GMG, the main features

used included a full approximation scheme (FAS) [24,25], V-cycle, and a grid-size ratio of 2. For both multigrid methods, lexicographic Gauss-Seidel [28] was employed as a smoother (with one internal iteration); the number of cycles was high enough to achieve the machine round-off error; double-precision operations were used for all the calculations; and a null temperature was employed for the whole domain as an initial guess.

While for the primary variable of interest the adopted approximation scheme was the CDS, for other variables of interest (specially the global ones), other schemes/techniques had to be employed. Therefore, to numerically evaluate the integrals related to the average temperature of the whole domain and the heat transfer rates at the four boundaries, the rectangle rule [29] was employed. Moreover, for the evaluation of  $Q_e$ , the upstream differencing scheme (UDS) [5,18] was used to numerically approximate the derivatives (Eq. (3)); for  $Q_s$ , the downstream differencing scheme (DDS) [5,18] was employed for the same purpose. In both cases, these approximations were employed while always using the numerical results for the nodal temperatures (the primary variable of interest) previously obtained. Otherwise, the temperature at the domain center was evaluated by determining the arithmetical average of the temperatures of the volumes with one of the vertices at the coordinates  $x = 1/2$  and  $y = 1/2$ . This procedure was needed once neither the triangular nor the square grids featured a nodal point that was located exactly at the domain geometric center.

According to the results reported by Marchi and Germer [13], it is clear that RRE can behave in different ways depending on the type of variable: local vs. global or primary (the dependent variable  $T$  in the partial differential equation) vs. secondary (a variable that is derived from a primary one). Hence, it is important to study RRE for different types of variables. Thus, each variable of interest was chosen for the following reasons:  $T_c$  involves the arithmetic average of the temperature at the neighbor control volumes to evaluate the temperature at the domain center;  $T_m$  involves the rectangle rule for numerical integration; and  $Q_e$  and  $Q_s$  involve the UDS and DDS for the evaluation of their derivatives and the rectangle rule for their integrations.

### 3.2. Numerical solutions with RRE

Once the numerical solutions are obtained, according to the Section 3.1, Richardson extrapolations can be used to reduce the numerical errors associated with the discretization process according to the following expression:

$$\phi_{g,m} = \phi_{g,m-1} + \frac{\phi_{g,m-1} - \phi_{g-1,m-1}}{r^{p_{m-1}} - 1}, \quad (8)$$

where  $\phi$  is the numerical solution of a given variable of interest; the index  $g$  refers to the grid on which the numerical solution is evaluated; the index  $m$  is the number of Richardson extrapolations;  $p_m$  are the true orders of the discretization error [4]; and  $r$  is the refinement ratio ( $r = h_{g-1}/h_g$ ), where

$$h = (A/N)^{1/2} \quad (9)$$

is the reference size of the control volumes employed for the domain discretization. In Eq. (9),  $A$  is the whole domain area and  $N$  is the total number of volumes into which the domain is split. As seen in Eq. (9), the grid type (triangular or square) does not influence the value of  $h$ . For three-dimensional problems, the area  $A$  should be replaced by the volume  $V$  of the entire domain, while the power  $1/2$  should be replaced by  $1/3$ . In practice, the total area or the total volume for two- and three-dimensional problems, respectively, are evaluated by the summation of the area or the volume related to each control volume of the adopted grid.

Equation (8) is valid for  $g = [2, G]$  and  $m = [1, g-1]$ , where  $g = 1$  refers to the coarsest grid,  $g = G$  is the most refined grid,  $m = 0$  refers to the numerical solution without any extrapolation and  $m = 1$  is related to the standard Richardson extrapolation. For each value of  $\phi_{g,m}$  in Eq. (8), numerical solutions of  $\phi$  on two different grids ( $g$  and  $g-1$ ) for the  $m-1$  extrapolation are needed.

For a given value of  $g$ , Eq. (8) can be used recursively  $g-1$  times, providing  $m$  Richardson extrapolations. In the current work, RRE results are obtained when  $m > 1$ . The values of the true orders ( $p_m$ ) are related to the exponents of the truncated terms of the Taylor series employed in the approximation schemes for the derivatives. More details about Eq. (8) and/or RRE theory are presented by Marchi et al. [12].

## 4. Numerical results

Two different domain geometries are employed in the current work. The first one consists of a unitary square domain, which is discretized into an isosceles right-triangular or square grid, and the results are presented and analyzed in Sections 4.1–4.4. The second geometry, a half square triangle, and its results are described in Section 4.5 to verify whether the numerical results obtained for the first domain geometry can be directly applied to other geometries.

### 4.1. Consistency of triangular and square grids

Twelve different grids are employed in the current work for both triangular and square grids: from grids with only 4 real volumes ( $2^2$ ) up to 16,777,216 real volumes ( $2^{24}$ ), respecting a (two-dimensional) refinement ratio of 2. Double precision was used for all operations, and the number of multigrid cycles for both grid geometries was high enough to minimize

the iteration error. The numerical results for the six variables of interest are compared to the values of the analytical solutions, with 30 significant figures, obtained with quadruple precision. These comparisons allow for the evaluation of the real numerical error in order to study the efficiency of RRE to reduce the numerical errors.

For all numerical simulations, the number of multigrid cycles was kept high enough to achieve the machine round-off error. In this case, the iteration error was at least 6 orders of magnitude smaller than the discretization error. It was verified by the observation of the  $l_1$ -norm, which decreased by at least 12 orders of magnitude and began to present oscillatory behavior. This procedure was used to guarantee that the magnitude of all the other error sources was much smaller than the discretization one and thereby allow the use of the Richardson extrapolations and, consequently, the RRE methodology.

The consistency of both the triangular and square volumes can be observed in Fig. 3: as expected, for both cases, the mean  $l_1$ -norm of the numerical error of the temperature decreases with grid refinement ( $h$  represents the two-dimensional grid spacing). Considering the same number of volumes for both triangular and square grids, Fig. 3 shows that the mean  $l_1$ -norm is always higher on triangular grids in comparison to the square counterparts by a factor of approximately 2.3–2.4 (excepted by the two coarsest grids). This result is in agreement with that reported by Juretić and Gosman [19], in whose work it was observed that square grids provide the most accurate numerical results for two-dimension problems.

#### 4.2. Apparent orders using RRE

The use of several grid sizes allows for the evaluation of apparent orders ( $p_U$ ) for all the variables of interest. Apparent orders [30] should be used for the *a posteriori* verification of the values obtained *a priori* for the true orders of the numerical error. Details about the evaluation of the true orders and their use in the RRE methodology are explained by Marchi et al. [12].

The results of the apparent orders ( $p_U$ ) for the heat transfer rate at  $x = 1$  ( $Q_e$ ) for both grid volume geometries are presented in Fig. 4. When  $m = 0$ , the results are related to the asymptotic error order, while for  $m = 1$  and  $m = 2$ , the results

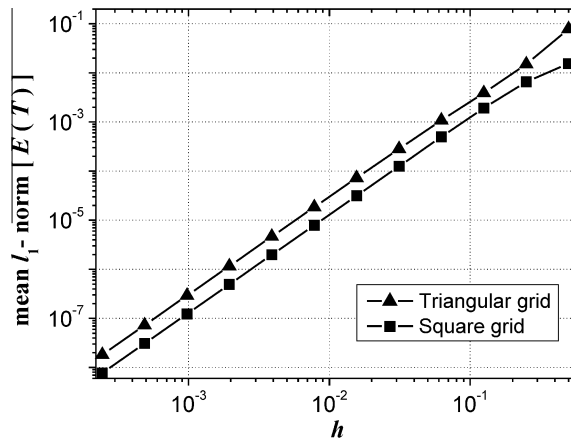


Fig. 3. Mean  $l_1$ -norm of the numerical error  $E(T)$  without RRE versus  $h$ . Unitary square domain.

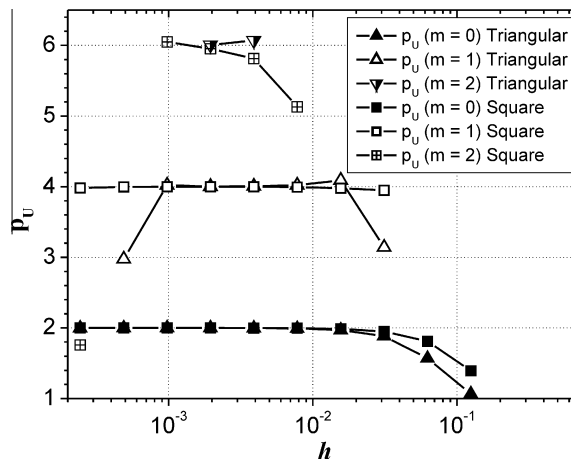


Fig. 4. Apparent orders versus  $h$  for  $Q_e$ . Unitary square domain.

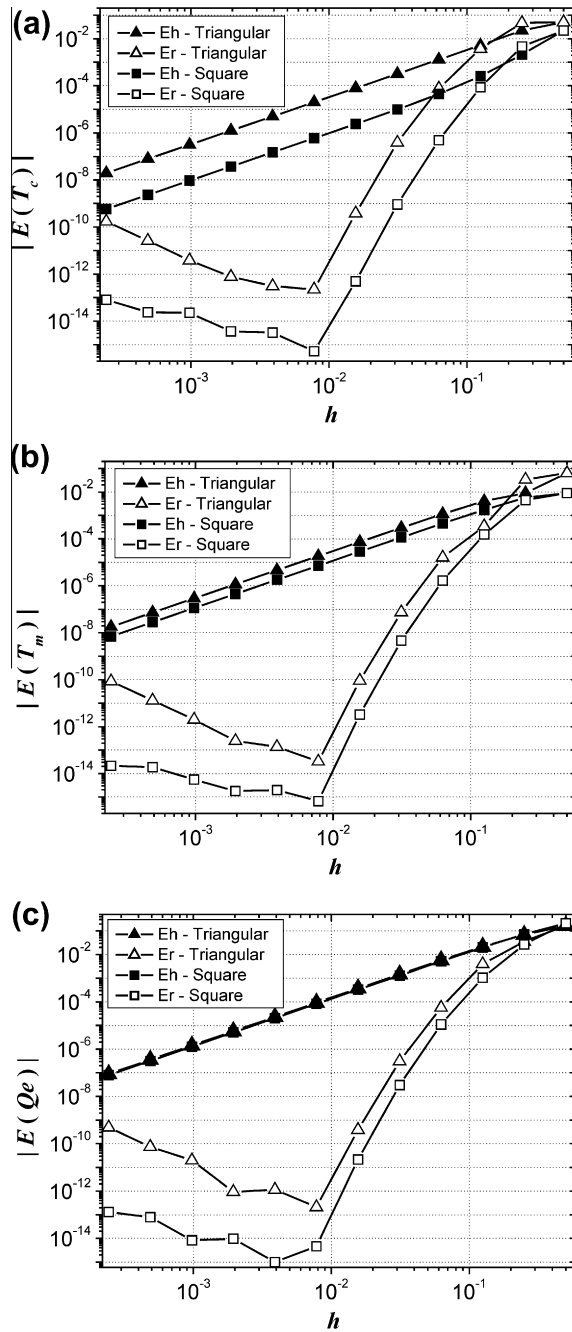


Fig. 5. Modulus of the numerical error with (Er) and without (Eh) RRE versus  $h$  for (a)  $T_c$ ; (b)  $T_m$ ; (c)  $Q_e$ . Unitary square domain.

are related to the second and third true error orders, respectively. Apparent orders tend to assume values of 2, 4 and 6, in accordance with the results presented by Giacomini and Marchi [31] for the first-order approximations (UDS) of derivatives. This result, however, comes from a type of order degeneration, when the UDS presents an asymptotic error order of unitary value and not of a value of 2. Nevertheless, because the apparent orders tend to 2, 4, 6 and so on, these values were employed as true orders for RRE. Similar behavior was observed for the other heat transfer rates ( $Q_n, Q_s, Q_w$ ) and for the other variables of interest ( $T_c, T_m$ ), although for these two, the expected true order values were those that were found.

#### 4.3. Triangular grid versus square grid

The discretization error results for the variables of interest are presented in Fig. 5. The numerical results for the heat transfer rates at  $y = 0$  ( $Q_s$ ),  $y = 1$  ( $Q_n$ ) and  $x = 0$  ( $Q_w$ ) are similar to those for the heat transfer rate at  $x = 1$  ( $Q_e$ ) and are,

therefore, omitted. In all cases, the results for both the triangular and square grids are presented, where  $E_h$  is the numerical error without RRE and  $E_r$  is the numerical error with RRE. As anticipated by the  $l_1$ -norm (Fig. 3), in every case, the numerical errors observed, without RRE, on square grids are smaller than their counterparts on triangular grids. Even for  $Q_e$ , Fig. 5(c), the square grid results are slightly better than those for the triangular grids, although the curves for both are almost coincident.

Considering the results for the grid with  $2^{14} = 16,384$  volumes ( $h \approx 8 \times 10^{-3}$ ) on triangular grids, it can be seen in Fig. 5 that the numerical errors are under  $10^{-12}$  for all the variables when RRE is employed. In comparison, taking the same grid, but not employing RRE, the numerical errors are approximately  $10^{-4}$  or  $10^{-5}$ . In this case, the use of RRE could reduce numerical errors by approximately 7 or 8 orders of magnitude, proving the efficiency of RRE in reducing the numerical error in triangular grids. This effect is similar to that observed for square grids: taking the same grid (with 16,384 volumes), the numerical error without RRE is approximately  $10^{-4}$  to  $10^{-6}$ , while the use of RRE provides numerical errors of approximately  $10^{-14}$  or  $10^{-15}$ . Comparing both results, the use of RRE could reduce numerical errors by approximately 8 to 10 orders of magnitude, as previously observed by Marchi et al. [12] and Marchi and Germer [13].

The better performance of RRE on square grids, when compared to that on triangular ones, can be related to two factors: (1) triangular grids present higher magnitudes of discretization errors, caused by the mesh skewness for two of the triangle sides [18,19], considering the grid arrangement; and (2) triangular grids also present higher magnitudes of machine round-off errors when a higher number of arithmetic operations are needed to evaluate the coefficients, which is more appreciable for refined grids.

#### 4.4. Further comparisons of numerical results with and without RRE

One of the possible uses of RRE is clearly illustrated in Table 1: for a given error magnitude, the use of the RRE methodology allows for the use of coarser grids, when compared to the numerical results obtained without RRE. The analyzed unknown is the temperature at the domain center ( $T_c$ ); other unknowns, however, present a similar behavior. The effects of RRE on reducing the numerical error become more appreciable for smaller error magnitudes, on both triangular and square grids. Table 1 clearly shows how the ratio between the number of volumes needed to provide a given error magnitude with and without RRE rapidly increases with the number of extrapolations. For example, on triangular grids, if the error magnitude is fixed at approximately  $1 \times 10^{-4}$ , the observed ratio presents a value of 4 (associated to 3 extrapolations); for a smaller error magnitude, at approximately  $2 \times 10^{-8}$ , this ratio achieves a value of 4096 (associated to 5 extrapolations). This effect is also observed on square grids, and it is in agreement with the results presented by Marchi et al. [12] and Marchi and Germer [13].

The results presented in Table 1 also show that although RRE is efficient in reducing the number of control volumes necessary to achieve a given numerical error level on both triangular and square grids, the chosen grid type influences the required grid refinement. For each of the numerical error magnitudes presented in Table 1, it is observed that when using RRE,

**Table 1**

RRE performance for given error magnitudes for  $T_c$ .

Error magnitude	$E \approx 1 \times 10^{-4}$	$E \approx 1 \times 10^{-6}$	$E \approx 2 \times 10^{-8}$
Triangular grid without RRE	$2^{10} = 1024$	$2^{18} = 262,144$	$2^{24} = 16,777,216$
Triangular grid with RRE	$2^8 = 256$	$2^{10} = 1024$	$2^{12} = 4096$
Number of extrapolations (triangular grid)	3	4	5
Ratio between the number of volumes without and with RRE (triangular grid)	4	256	4096
Square grid without RRE	$2^6 = 64$	$2^{14} = 16,384$	$2^{18} = 262,144$
Square grid with RRE	$2^6 = 64$	$2^8 = 256$	$2^{10} = 1024$
Number of extrapolations (square grid)	2	3	4
Ratio between the number of volumes without and with RRE (square grid)	1	64	256
Ratio between the number of volumes on triangular and square grids (both results with RRE)	4.0	4.0	4.0

**Table 2**

RRE performance for given grid sizes for  $T_c$ .

Number of volumes	$2^6 = 64$	$2^{10} = 1024$	$2^{14} = 16,384$
Error magnitude on triangular grid and without RRE	$5.20 \times 10^{-3}$	$3.20 \times 10^{-4}$	$2.00 \times 10^{-5}$
Error magnitude on triangular grid and with RRE	$3.73 \times 10^{-3}$	$3.83 \times 10^{-7}$	$2.25 \times 10^{-13}$
Number of extrapolations (triangular grid)	2	4	6
Ratio between the numerical error without and with RRE (triangular grid)	1.39	$8.36 \times 10^2$	$8.89 \times 10^7$
Error magnitude on square grid and without RRE	$2.52 \times 10^{-4}$	$9.90 \times 10^{-6}$	$5.95 \times 10^{-7}$
Error magnitude on square grid and with RRE	$8.53 \times 10^{-5}$	$9.17 \times 10^{-10}$	$5.27 \times 10^{-16}$
Number of extrapolations (square grid)	2	4	6
Ratio between the numerical error without and with RRE (square grid)	2.95	$1.08 \times 10^4$	$1.13 \times 10^9$
Ratio between the error magnitude on triangular grid and the error magnitude on square grid (both results without RRE)	$2.06 \times 10^1$	$3.23 \times 10^1$	$3.36 \times 10^1$
Ratio between the error magnitude on triangular grid and the error magnitude on square grid (both results with RRE)	$4.37 \times 10^1$	$4.18 \times 10^2$	$4.27 \times 10^2$

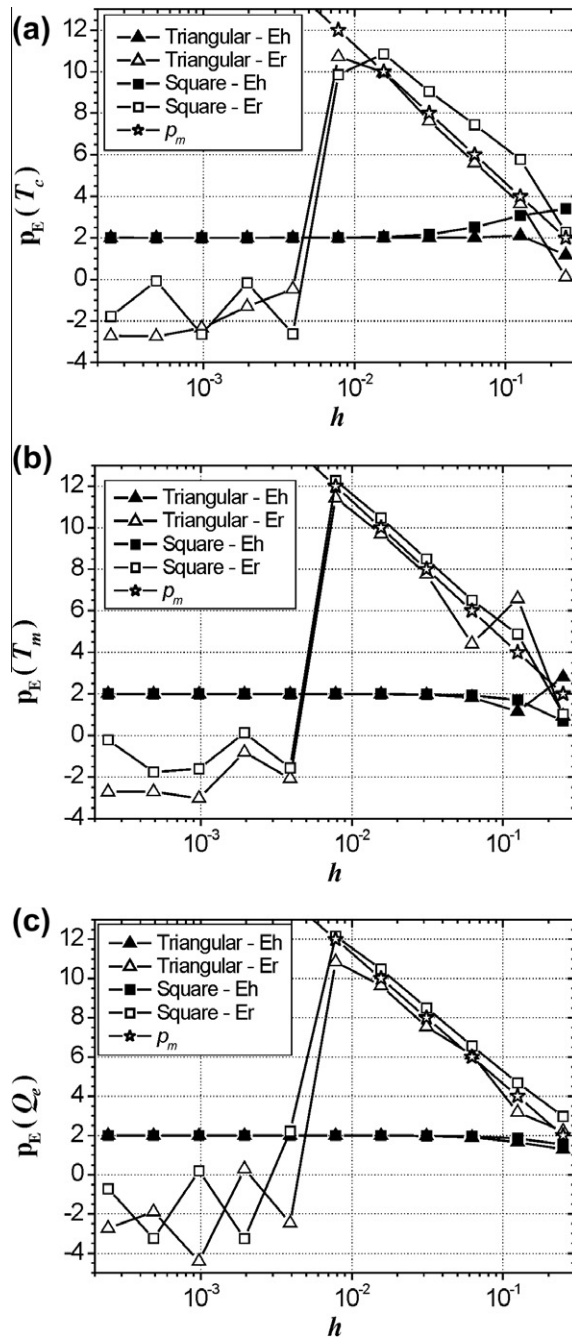


Fig. 6. Effective orders for the numerical errors of Fig. 5 (unitary square domain).

a specific triangular grid always presented four times more volumes than the analogous square grid in achieving the same level of numerical error. This result is attributed to the higher discretization error levels associated with the triangular grid when compared to the square one, as reported by Juretić and Gosman [19].

Another possible use of RRE is illustrated in Table 2: in this case, the grid sizes were fixed and the numerical error associated with these grids was evaluated for  $T_c$ . Once again, the behavior of other variables of interest is similar to that presented. Table 2 shows that the ratio between the numerical errors observed without the use of RRE and those observed with RRE expands quickly with the increase in the number of volumes, a fact which is related to the increase in the number of extrapolations.

From Tables 1 and 2 and Fig. 5(a), it is observed that on both grid types the use of RRE quickly reduces the error magnitude, except that for the coarsest grids, for which the RRE performance is not appreciable. This behavior is expected because

the RRE methodology becomes more efficient with the increase in the number of extrapolations, which is achieved with grid refinement. The reduction of the numerical error is accelerated with the increase in the number of extrapolations until the machine round-off error ( $\approx 10^{-13}$ ) is achieved, which is compatible with the employed precision (in the current work, double precision).

Table 2 also presents information regarding the ratio between the numerical error magnitudes on triangular and square grids, with and without the use of RRE. For the same number of control volumes, the numerical error associated with triangular grids is approximately 32–33 times that observed in an analogous square grid, without the use of RRE. An exception is observed when only  $2^6 = 64$  volumes are employed: this ratio is approximately 20 times. Such behavior, however, can be explained by once again observing the results presented in Fig. 4: the apparent orders for both triangular and square grids are not close enough to the asymptotic value of 2 on the 64-control-volume grid. Thus, the ratio between the numerical errors of the two grid types presents a different value than that obtained when asymptotic behavior is achieved.

A similar effect is also observed when RRE is employed: while on the 64-control-volume grid, the ratio between the numerical errors in the two grid types is approximately 43.7; when the results for more-refined grids are compared, this ratio achieves a value of over 400, despite the fact that RRE is effective in reducing the numerical error in each grid type. From these results, it is again observed that the numerical errors associated with the triangular grid are larger than those obtained for a corresponding square grid, as predicted by Juretić and Gosman [19].

The rapid reduction in numerical errors achieved by the use of the RRE is related to the increase in the effective orders of the solutions for all the variables. These orders are related to the fact that when the numerical error consists of only truncation error (in which case it is called discretization error), it can be represented by [28] the following:

$$E(\phi) = C_0 h^{p_0} + C_1 h^{p_1} + C_2 h^{p_2} + \dots = \sum_{m=0}^{\infty} C_m h^{p_m}, \tag{10}$$

where  $C_0, C_1, C_2, \dots$  are coefficients that are independent of  $h$ ; and  $p_0, p_1, p_2, \dots$  are the true orders of  $E(\phi)$ , whose set is represented by  $p_m$ . The values of  $p_m$  are generally positive integers [32], consisting of an arithmetic progression, where  $0 < p_0 < p_1 < p_2 < \dots$ , and can be evaluated by the following:

$$p_m = p_0 + m(p_1 - p_0), \tag{11}$$

where  $p_0$  the asymptotic order of the error and  $m$  the number of Richardson extrapolations. Equation (11) is valid for  $g = [1, G]$  and  $m = [0, g - 1]$ .

The increase in the effective orders on both triangular and square grids is presented in Fig. 6 for the temperature at the domain center ( $T_c$ ), the average temperature of the whole domain ( $T_m$ ), and the heat transfer rate at the  $x = 1$  boundary ( $Q_e$ ). The other variables of interest, however, present similar behavior. To provide a better analysis of the efficiency of RRE, the true orders ( $p_m$ ) are also presented. As seen in Fig. 6, the use of RRE increases the effective order to values over 10 on both triangular and square grids. These effective orders present values close to the expected ones (true orders) and asymptotically tend to the  $p_m$  values with the grid refinement. This behavior, however, is only observed until the machine round-off error is achieved, which influences and degenerates the order results. Comparing the values plotted in Figs. 5 and 6, it is seen that the minimum values for the numerical errors correspond to the maximum values of the effective orders, which are as high as 12.

As previously mentioned in Section 4.1, in the current work, the adopted grid refinement ratio was equal to 2. However, it must be observed that this is not always necessary. If there is an interest in obtaining several extrapolations for coarse grids, a grid refinement ratio with a value close to unity can be employed. However, it is known that Richardson extrapolations present better results for refined grids. The use of RRE on coarse grids needs to be further investigated: good results for these grids would allow for the use of RRE in practical CFD problems, in which grids are relatively coarse.

Another remark that can be made about the adopted grid refinement is related to the fact that there is no coincidence among the positions of the nodal points on different grids. This fact, however, does not seem to have any effect on either

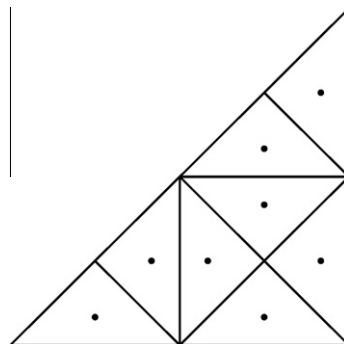


Fig. 7. Half square triangle domain with 8 control volumes.

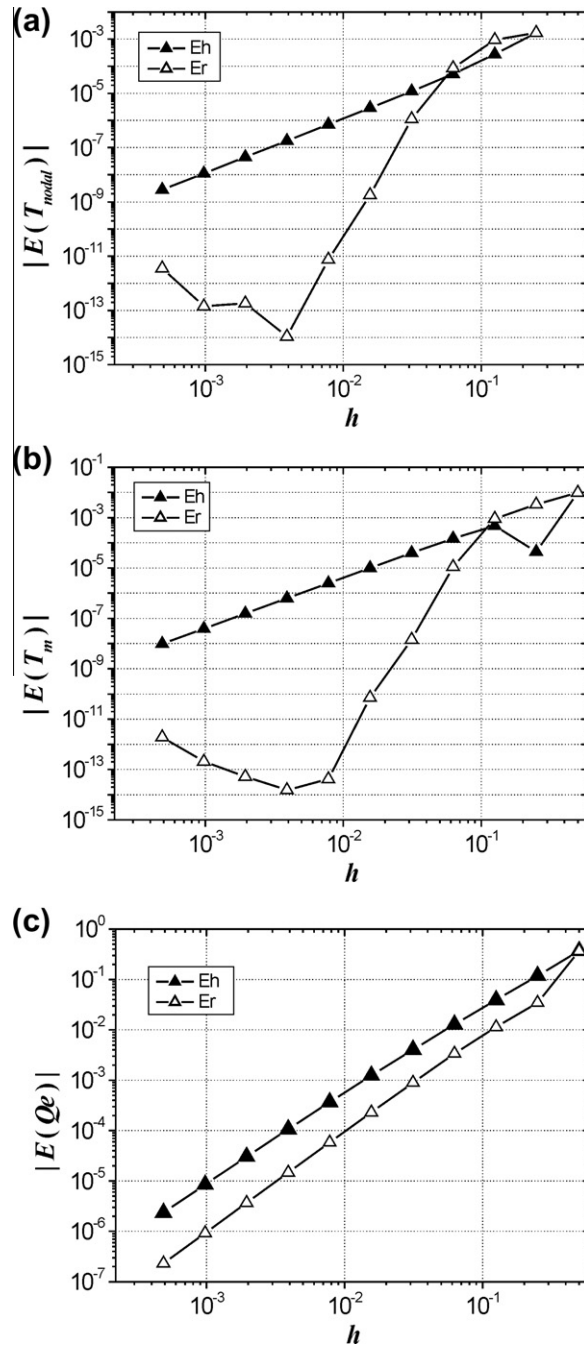


Fig. 8. Modulus of the numerical error with (Er) and without (Eh) RRE versus  $h$  for (a)  $T_{nodal}$ ; (b)  $T_m$ ; (c)  $Q_e$ . Half square triangle domain.

numerical behavior or RRE performance: such effects are more closely related to variable type – global or local. Global variables of interest, such as  $T_m$  and  $Q_e$ , are not affected by the absence of coincident nodal points: as seen in Fig. 4 for  $Q_e$ , the evaluated apparent orders correspond to the expected true orders. This is because global variables of interest involve numerical results for several grid nodes and, because of this, eventual new discretization error terms can be mutually canceled by summing them during the numerical integration process. In contrast, for local variables of interest, the efficiency of the RRE methodology is related to the asymptotic behavior of the numerical solutions. If this behavior is not observed, Richardson extrapolations cannot be applied [33]. Fortunately, for all local variables of interest studied in the current work, this asymptotic behavior was observed; otherwise, a technique that allows the numerical solution to present asymptotic behavior should be used.

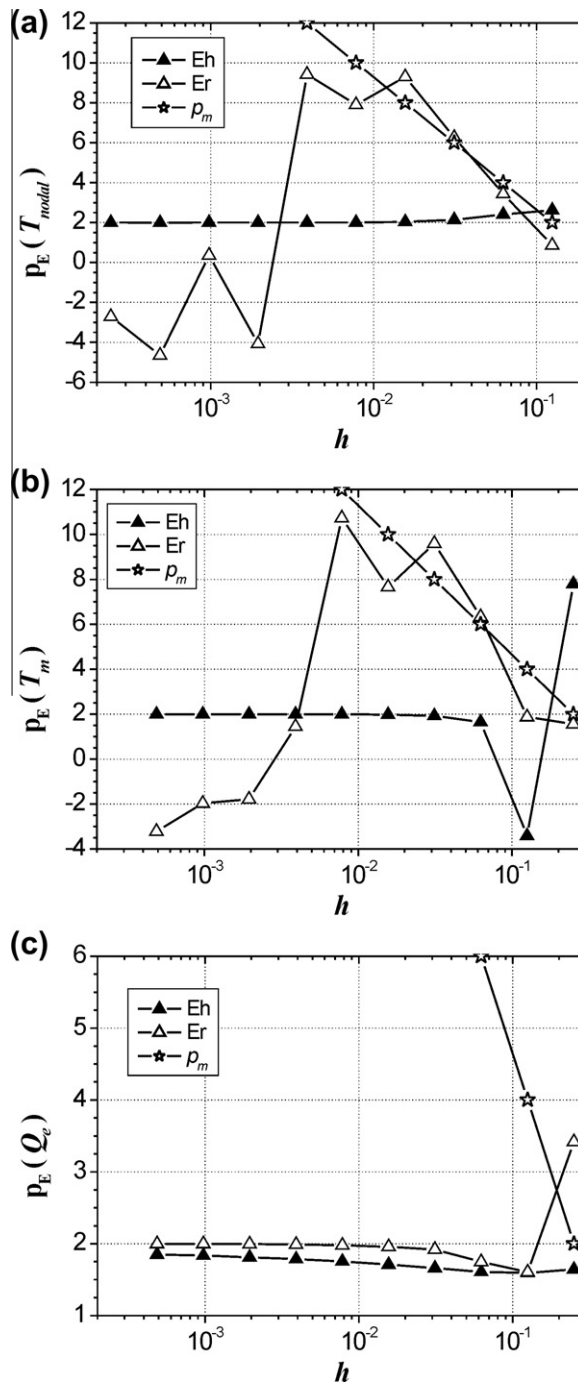


Fig. 9. Effective orders for the numerical errors of Fig. 8 (half square triangle domain).

To summarize, the use of RRE is efficient for the reduction of numerical error in both triangular and square grids. Its performance is much better than that of a simple grid refinement and is limited only by the machine round-off errors, which depends on a series of variables (such as the algorithm of the numerical code, hardware and software). For both grid types, the use of RRE was effective for grids with up to  $2^{14} = 16,384$  volumes ( $h \approx 8 \times 10^{-3}$ ) at maximum; for more-refined grids, the machine round-off errors became the dominant term in the numerical error. As a consequence, although the discretization error decreases with the grid refinement, the machine round-off error increases with it such that the numerical error always presents a minimum value [34]. In this case, for more refined grids, even if the RRE methodology reduces the discretization error, the numerical error tends to increase when the machine round-off error presents a higher magnitude. Such a

situation can be avoided by using quadruple precision, whose round-off error is approximately  $10^{-30}$ – $10^{-32}$ , as demonstrated by Marchi et al. [12].

#### 4.5. A second domain geometry: a half square triangle

In this case, a domain geometry consisting of a half square triangle (Fig. 7) was also employed to provide other results regarding the efficiency of the RRE methodology for triangular grids. The studied mathematical model is based on the two-dimensional Laplace equation with Dirichlet boundary conditions:

$$\begin{cases} \frac{\partial^2 T}{\partial x^2} + \frac{\partial^2 T}{\partial y^2} = 0, & 0 < y < x, \quad 0 < x < 1, \\ T(x, y = x) = \sin(\pi x) \frac{\sinh(\pi x)}{\sinh(\pi)}, \quad T(1, y) = T(x, 0) = 0. \end{cases} \quad (12)$$

For this new geometry, the analytical solution for the temperature field is the same as that for the first geometry,  $T(x, y) = \sin(\pi x) \sinh(\pi y) / \sinh(\pi)$ . Other variables of interest for this second geometry are the following: (1) the temperature at position  $x = 3/4$  and  $y = 1/4$  ( $T_{nodal}$ ); (2) the average temperature ( $T_m$ ) of the whole domain; and the heat transfer rates on the three boundaries, namely: (3)  $y = 0$  ( $Q_s$ ), (4)  $x = 1$  ( $Q_e$ ), and (5)  $x = y$  ( $Q_i$ ). For this geometry, only triangular grids were employed, retaining the same discretization procedures adopted for the first domain geometry (square domain, discretized with triangular grids).

Eleven different grids are employed for this new geometry, starting with the coarsest one, with 2 real control volumes, and ending with the finest one, with 2097,152 real control volumes ( $2^{21}$ ), respecting a (two-dimensional) refinement ratio of 2. The RRE methodology was applied to all the variables of interest. As seen in Fig. 8(a) and (b), the RRE methodology was efficient in reducing the discretization error for two types of variables of interest: the nodal temperature ( $T_{nodal}$ ) at  $x = 3/4$  and  $y = 1/4$  and the average temperature of the entire domain ( $T_m$ ). The performance of RRE with respect to these two variables was as expected, based on the previously presented results: RRE could reduce the numerical errors by approximately 6 to 8 orders of magnitude for a grid with 32,768 control volumes. Unfortunately, however, for the heat transfer rates, the expected behavior was not observed. Only  $Q_e$  is presented in Fig. 8 because  $Q_s$  and  $Q_i$  exhibit similar behavior. Although the use of RRE reduced the numerical discretization error for this kind of variable, the RRE performance for this kind of variable was much smaller than the expected one, as seen in Fig. 8(c): the numerical errors were reduced by only a factor of about 10 (one order of magnitude).

The increase in the effective orders for  $T_{nodal}$ ,  $T_m$  and  $Q_e$  are presented in Fig. 9. As seen, for this second domain geometry, the expected behavior for the increase in the effective orders occurred only for  $T_{nodal}$  and  $T_m$  (Fig. 9(a) and (b)). For these variables, the effective orders increase with the grid refinement until the grid contains 2048 control volumes. However, when the grid contains 32,768 control volumes, the effective orders are not negative: these results are most likely adversely affected by the round-off errors. For more-refined grids (131,072 control volumes and so on), the machine round-off error becomes the most important component of the numerical error and therefore RRE is no longer effective in reducing the numerical error. For the heat transfer rates, such as  $Q_e$  (Fig. 9(c)), however, the increase in the effective orders is not observed for the half square triangle domain: RRE only accelerates the tendency of the effective order to approach the asymptotic value of 2. The reasons why RRE is not effective for this kind of variable of interest in the second employed geometry is not yet clear and requires supplementary studies, which are in progress. One hypothesis for this degradation in RRE performance for the heat transfer rates is related to the application of boundary conditions. For this second domain geometry and for the chosen discretization, there is an extra component of the discretization error related to the fact that, for at least one of the boundaries, the line that connects the centroids of the real and the ghost cells does not pass exactly through the mid-face. This new discretization error component could be attenuated somehow for nodal and global variables of interest but could be effective for variables of interest that are located exactly on the boundaries, such as the heat transfer rates.

## 5. Conclusion

Isosceles right-triangular (for two domain geometries: unitary square and half square triangle) and square grids (for a unitary square domain) were employed for the discretization of a two-dimensional Laplace equation with Dirichlet boundary conditions by the finite volume method to study the efficiency of RRE. The implemented numerical model features a second-order approximation scheme (CDS); boundary conditions applied with ghost-cells; discretization with triangular grids according to the methodology for unstructured grids; discretization with square grids according to the procedures for structured grids; an algebraic multigrid for triangular grids and a geometric multigrid for square ones to speed up the numerical convergence; a lexicographic Gauss-Seidel smoother; a sufficiently high number of multigrid cycles to achieve the machine round-off error; and double-precision calculations.

The main results of the current work are as follows:

- (1) RRE is efficient in reducing numerical errors in triangular grids, achieving effective orders for the numerical error of approximately 11.

- (2) Despite the versatility of triangular grids, the use of square grids is recommended (if the geometry of the domain allows its use) due to the smaller discretization errors associated with this grid type. This result is in accordance with the results presented by Juretić and Gosman [19]. The current work also extends these results for the case in which RRE is employed.
- (3) Considering different grid types but using the same approximation scheme, the RRE results depend on the numerical error without extrapolation: the numerical error becomes smaller on square grids before implementing the RRE methodology; after implementing RRE, the numerical error remains smaller on square grids when compared that on triangular ones.
- (4) The numerical results also suggest that the use of RRE is efficient for other grid types, such as non-orthogonal ones.
- (5) It must be noted, however, that the efficiency of RRE is not the same for all variables of interest and all domain geometries: although the numerical error was reduced, the expected behavior of RRE was not observed in all cases (particularly for the variables of interest located at the domain boundaries).

The theoretical basis of RRE and the results reported in other studies [6–8,12,13,35] allow us to state that the results of the present work also apply, among others, to two- and three-dimensional Laplace, Poisson, Burgers and Navier-Stokes equations, as well as to unsteady problems. However, for some of the variables of interest at specific domain geometries, RRE cannot achieve its theoretical efficiency.

### Acknowledgements

The authors would like to acknowledge the financial support provided by CNPq (Conselho Nacional de Desenvolvimento Científico e Tecnológico - Brazil), AEB (Agência Espacial Brasileira, by the Uniespaço Program), Fundação Araucária (Paraná - Brazil), and CAPES (Coordenação de Aperfeiçoamento de Pessoal de Nível Superior - Brazil). The first author is supported by a CNPq scholarship. The fourth and fifth authors are grateful for the financial support provided by CAPES. The authors would also like to acknowledge Dr. K. Stüben for providing his algebraic multigrid (AMG) code, which was used as the basis for the AMG employed in the current work. The authors would also like to acknowledge the excellent suggestions provided by the referees and the editors.

### References

- [1] R.G. Ghanem, Uncertainty quantification in computational and prediction science, *Int. J. Numer. Methods Eng.* 80 (2009) 671–672.
- [2] L.F. Richardson, The approximate numerical solution by finite differences of physical problems involving differential equations with an application to the stresses in a masonry dam, *Philos. Trans. R. Soc. London A* 210 (1910) 307–357.
- [3] L.F. Richardson, J.A. Gaunt, The deferred approach to the limit, *Philos. Trans. R. Soc. London A* 227 (1927) 299–361.
- [4] C.H. Marchi, A.F.C. Silva, Unidimensional numerical solution error estimation for convergent apparent order, *Numer. Heat Transfer B* 42 (2002) 167–188.
- [5] J.C. Tannehill, D.A. Anderson, R.H. Pletcher, *Computational Fluid Mechanics and Heat Transfer*, second ed., Taylor & Francis, Philadelphia, 1997.
- [6] A.S. Benjamin, V.E. Denny, On the convergence of numerical solutions for 2-D flows in a cavity at large Re, *J. Comput. Phys.* 33 (1979) 340–358.
- [7] R. Schreiber, H.B. Keller, Driven cavity flows by efficient numerical techniques, *J. Comput. Phys.* 49 (1983) 310–333.
- [8] E. Erturk, T.C. Corke, C. Gökçöl, Numerical solutions of 2-D steady incompressible driven cavity flow at high Reynolds numbers, *Int. J. Numer. Methods Fluids* 48 (2005) 747–774.
- [9] Y. Wang, J. Zhang, Sixth order compact scheme combined with multigrid method and extrapolation technique for 2D Poisson equation, *J. Comput. Phys.* 228 (2009) 137–146.
- [10] Y.-M. Wang, H.-B. Zhang, Higher order compact finite difference method for systems of reaction-diffusion equations, *J. Comput. Appl. Math.* 233 (2009) 502–518.
- [11] Y. Ma, Y. Ge, A high order finite difference method with Richardson extrapolation for 3D convection diffusion equation, *Appl. Math. Comput.* 215 (2010) 3408–3417.
- [12] C.H. Marchi, L.A. Novak, C.D. Santiago, Multiple Richardson extrapolations to reduce and to estimate the discretization error of the two-dimensional Laplace equation (in Portuguese), in: *Proceedings of XIX Iberian-Latin-American Congress on Computational Methods in Engineering (CILAMCE)*, Maceió, Brazil, 2008.
- [13] C.H. Marchi, E.M. Germer, Verification of one-dimensional advection-diffusion schemes with and without multiple Richardson extrapolations (in Portuguese), in: *Proceedings of XXX Iberian-Latin-American Congress on Computational Methods in Engineering (CILAMCE)*, Armação de Búzios, Brazil, 2009.
- [14] R. Ouellet, R.T. Bui, A new tool for solving industrial continuous optimization problems, *Appl. Math. Model.* 17 (1993) 298–310.
- [15] R. Biswas, J.E. Flaherty, D.C. Arney, An adaptive mesh-moving and refinement procedure for one-dimensional conservation laws, *Appl. Numer. Math.* 11 (1993) 259–282.
- [16] H. Koestler, U. Ruede, Extrapolation techniques for computing accurate solutions of elliptic problems with singular solutions, *Proc. Lect. Notes Comput. Sci.* 3039 (2004) 410–417.
- [17] S.J. Kamkar, A. Jameson, A.M. Wissink, V. Sankaran, Using feature detection and Richardson extrapolation to guide adaptive mesh refinement for vortex-dominated flows, in: *Proceedings of 6th International Conference on Computational Fluid Dynamics (ICCFD)*, St. Petersburg, Russia, 2010, pp. 219–224.
- [18] H.K. Versteeg, W. Malalasekera, *An introduction to Computational Fluid Dynamics: The Finite Volume Method*, second ed., Pearson Education Limited, Harlow, 2007.
- [19] F. Juretić, A.D. Gosman, Error analysis of the finite-volume method with respect to mesh type, *Numer. Heat Transfer B* 57 (2010) 414–439.
- [20] R. Jyotsna, S.P. Vanka, Multigrid calculation of steady, viscous flow in a triangular cavity, *J. Comput. Phys.* 122 (1995) 107–117.
- [21] F.P. Incropera, D.P. DeWitt, T.L. Bergman, A.S. Lavine, *Fundamentals of Heat and Mass Transfer*, sixth ed., John Wiley & Sons, New York, 2007.
- [22] S.R. Mathur, J.Y. Murthy, A pressure-based method for unstructured meshes, *Numer. Heat Transfer B* 31 (1997) 195–215.
- [23] J.W. Ruge, K. Stüben, Algebraic multigrid, in: S.F. McCormick (Ed.), *Frontiers of Applied Mathematics 3: Multigrid Methods*, SIAM, Philadelphia, 1987, pp. 73–132.
- [24] W.L. Briggs, V.E. Henson, S.F. McCormick, *A Multigrid Tutorial*, second ed., SIAM, Philadelphia, 2000.

- [25] U. Trottenberg, C. Oosterlee, A. Schüller, *Multigrid*, Academic Press, San Diego, 2001.
- [26] A. Brandt, Algebraic multigrid theory: the symmetric case, *Appl. Math. Comput.* 19 (1986) 23–56.
- [27] K. Stüben, A review of algebraic multigrid, *J. Comput. Appl. Math.* 128 (2001) 281–309.
- [28] R.L. Burden, J.D. Faires, *Numerical Analysis*, eighth ed., Cengage Learning - Brooks Cole, Florence, 2005.
- [29] E. Kreyszig, *Advanced Engineering Mathematics*, eighth ed., John Wiley & Sons, New York, 1999.
- [30] G. De Vahl Davis, Natural convection of air in a square cavity: a bench mark solution, *Int. J. Numer. Methods Fluids* 3 (1983) 249–264.
- [31] F.F. Giacomini, C.H. Marchi, Verification of how to apply the boundary conditions in one-dimensional problems using the finite volume method (in Portuguese), in: *Proceedings of XXX Iberian-Latin-American Congress on Computational Methods in Engineering (CILAMCE)*, Armação de Búzios, Brazil, 2009.
- [32] D.C. Joyce, Survey of extrapolation processes in numerical analysis, *SIAM Rev.* 13 (1971) 435–490.
- [33] P.J. Roache, Discussion: factors of safety for Richardson extrapolation (Xing, T., and Stern, F., 2010, *ASME, J. Fluid Eng.*, 132, p. 061403), *J. Fluids Eng.* 133 (2011) 115501.
- [34] S.C. Chapra, R.P. Canale, *Numerical Methods for Engineers*, fifth ed., McGraw Hill, New York, 2006.
- [35] C.H. Marchi, R. Suero, L.K. Araki, The lid-driven square cavity flow: numerical solution with a  $1024 \times 1024$  grid, *J. Braz. Soc. Mech. Sci. Eng.* 31 (2009) 186–198.